ARTICLES
PUBLISHED ONLINE: 16 AUGUST 2009 | DOI: 10.1038/NCHEM.331
nature chemistry

A bonding model for gold(I) carbene complexes

Diego Benitez[1], Nathan D. Shapiro[2], Ekaterina Tkatchouk[1], Yiming Wang[2], William A. Goddard III[1] and F. Dean Toste[2]*

The last decade has witnessed dramatic growth in the number of reactions catalysed by electrophilic gold complexes. Although proposed mechanisms often invoke the intermediacy of gold-stabilized cationic species, the nature of bonding in these intermediates remains unclear. Herein, we propose that the carbon–gold bond in these intermediates comprises varying degrees of both σ- and π-bonding; however, the overall bond order is generally less than or equal to one. The bonding in a given gold-stabilized intermediate, and the position of this intermediate on a continuum ranging from gold-stabilized singlet carbene to gold-coordinated carbocation is dictated by the carbene substituents and the ancillary ligand. Experiments show that the correlation between bonding and reactivity is reflected in the yield of gold-catalysed cyclopropanation reactions.

The unique reactivity of organogold intermediates[1] has recently enabled a wide variety of new carbon–carbon bond-forming reactions to be developed[2]. On the basis of the reactivity patterns that have emerged[3], several mechanistic pathways[4] and bonding models[5] for key intermediates have been proposed, including intermediates ranging from gold carbenes[6] to gold-stabilized carbocations[7]. In the last year, theoretical investigations[8] and experimental observations[9] have further polarized the discussion surrounding the carbenoid or cationic character of organogold species, mostly in support of their carbocationic character[10]. However, gold catalysis has been applied successfully to perform reactions that are traditionally carried out with carbenic systems[11–16]. Given this apparent lack of a consistent and clear understanding of the Au–CR_2^+ bond, we have performed a broad theoretical analysis on key intermediates relevant to gold(I) catalysis. Experimental results in support of our analysis are also presented.

The study of carbon–metal multiple bonds has been an area of intense discussion since their discovery. For example, after the detection of rhodium carbenoids, debate ensued as to the nature of the rhodium–carbon bond[17]. Although certain calculations and experiments showed that the rhodium–carbon bond order was close to one, eventually it was accepted, on the basis of reactivity, that a metal–carbon double bond[18] was a more useful and convenient descriptor[19]. A similar discussion has recently emerged concerning the nature of the gold–carbon bond. Although partially semantic, the correct description is useful for both predicting and explaining reactivity.

Results and Discussion

Barrier to bond rotation energy. The magnitude of rotational barriers is a practical way of estimating the strength of π-bonds. Fürstner and co-workers devised a clever experiment to evaluate the carbenic/carbocationic character of (*Z*)-$\mathbf{Au_O}^{\mathbf{PPh}}$ and (*Z*)-$\mathbf{Au_{OMe}}^{\mathbf{PMe}}$ (see Fig. 1 for explanation of notation) by measuring the rotational barrier of bonds adjacent to gold[10]. They concluded that the contribution of the 'carbene' resonance was marginal. We used Fürstner's experiments to validate our theoretical methodology based on the M06 functional[20] of density functional theory.

Recently, the M06 functional has been shown to accurately describe[21,22] transition-metal-catalysed organic transformations. To confirm this, we calculated rotational barriers for (*Z*)-$\mathbf{Au_O}^{\mathbf{PPh}}$ and (*Z*)-$\mathbf{Au_{OMe}}^{\mathbf{PMe}}$ (Fig. 1) and obtained $\Delta G^{\ddagger} = 10.6$ kcal mol^{-1} for (*Z*)-$\mathbf{Au_O}^{\mathbf{PPh}}$, which is in excellent agreement with experiment ($\Delta G^{\ddagger} = 11.0$ kcal mol^{-1}), and $\Delta G^{\ddagger} = 5.8$ kcal mol^{-1} for (*Z*)-$\mathbf{Au_{OMe}}^{\mathbf{PMe}}$, also consistent with experiment (<7.2 kcal mol^{-1}). Previous density functional theory studies[8] used either B3LYP or BP86 functionals. Although these methods have proven valuable for many organometallic studies, we find that they are insufficient to resolve the issues of interest here. For example, B3LYP predicts rotational barriers of $\Delta G^{\ddagger} = 9.1$ and 7.9 kcal mol^{-1}, whereas BP86 predicts $\Delta G^{\ddagger} = 8.9$ and 7.4 kcal mol^{-1} for (*Z*)-$\mathbf{Au_O}^{\mathbf{PPh}}$ and (*Z*)-$\mathbf{Au_{OMe}}^{\mathbf{PMe}}$, respectively. This suggests that both B3LYP and BP86 cannot resolve the effects of the more electron-donating PMe_3 from the less electron-donating PPh_3.

Using our validated computational method, we calculated the barriers to bond rotation for metal-free allyl cations **1**, **2**, and **3**, as well as the gold species (*Z*)-$\mathbf{Au_{Me}}^{\mathbf{PMe}}$. The results confirm the conclusion of Fürstner and co-workers[10] that the gold moiety has little effect on the barrier to rotation in (*Z*)-$\mathbf{Au_O}^{\mathbf{PPh}}$ (a difference of $\sim$1.4 kcal mol^{-1} between (*Z*)-$\mathbf{Au_O}^{\mathbf{PPh}}$ and **1**); however, this conclusion is only valid in the presence of the highly carbocation-stabilizing oxygen atoms. When these heteroatoms are absent, the effect of the gold moiety is quite large (a difference of $\sim$8.1 kcal mol^{-1} between (*Z*)-$\mathbf{Au_{Me}}^{\mathbf{PMe}}$ and **2**). For comparison, the highly stabilizing methoxy group in **3** increases the barrier to rotation to 8.9 kcal mol^{-1} higher than that of **2**.

These results suggest that the reactivity of a given gold-stabilized carbene is highly dependent upon the carbene substituents. To gain further insight into the nature of the gold–carbon bond, we examined the structures of these types of intermediates, while varying both the carbene and ancillary ligand substituents.

Impact of the carbene. As a basis for comparison, we began by calculating the structures and natural atomic charges[23] of metal-free allyl cations **4**, **5**, and **6** (Fig. 2a). We also defined parameter *A* as the ratio of the bond lengths: $A \equiv (C^1-C^2)/(C^2-C^3)$, so that *A* indicates roughly whether the partial positive charge on the substrate is more stabilized by its C^1 or C^3 substituents. The low value of *A* in **4** (0.926) is indicative of the stabilizing nature of the oxygen lone pairs. The magnitude of *A* increases with less-donating C^3-methyl

[1]Materials and Process Simulation Center, California Institute of Technology, Pasadena, California 91125, USA, [2]Department of Chemistry, University of California, Berkeley, California 94720, USA. *e-mail: fdtoste@berkeley.edu

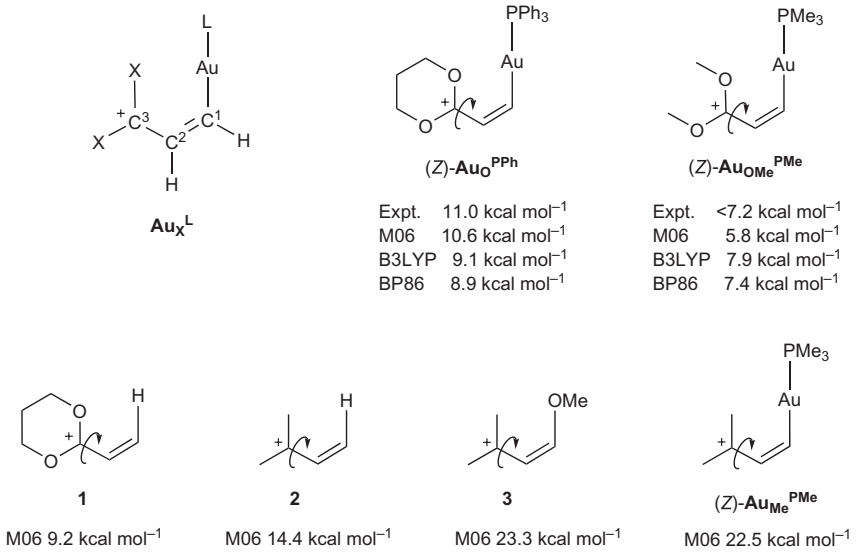

Figure 1 | Calculated and experimental activation energies to bond rotation (indicated with arrows). C^3–C^2 bond rotation barriers are decreased when C^3 is substituted with carbocation-stabilizing oxygen atoms. Throughout this article, gold complexes will be referred to according to the Au_X^L notation, where L indicates the ancillary ligand on gold and X indicates the C^3 substituents (Me = methyl, O = 1,3-dioxanyl, OMe = methoxy, E = methyl ester). M06, B3LYP and BP86 refer to the specific functional used in density functional theory calculations.

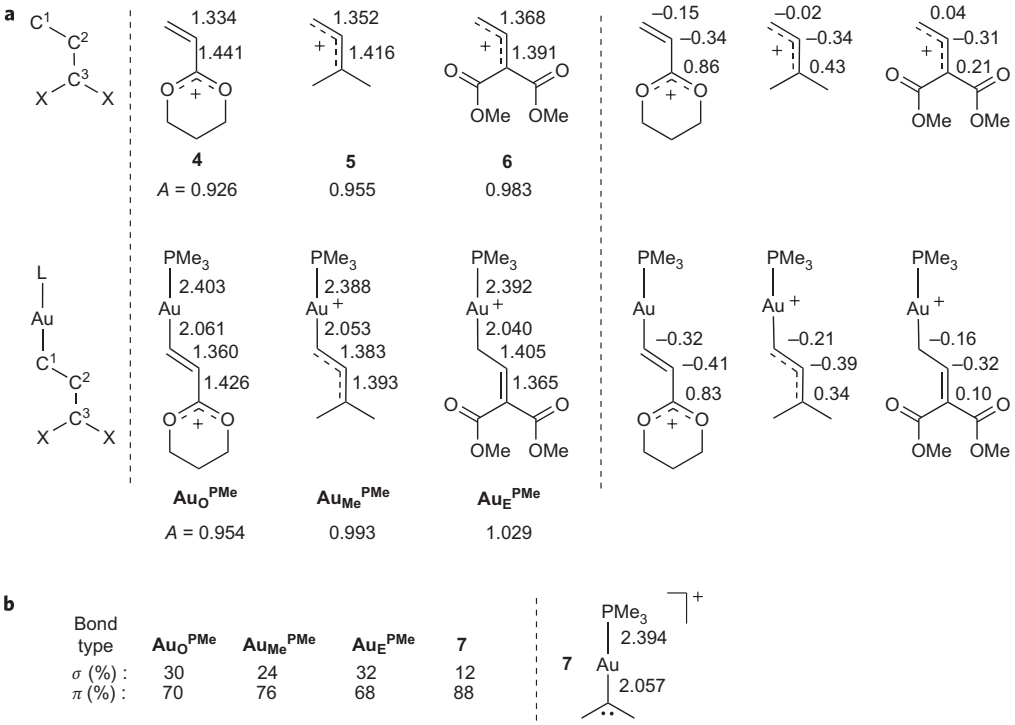

Figure 2 | Structural and electronic comparison of cationic metal-free and $[AuPMe_3]^+$ substituted substrates. a, On the left, calculated bond distances (Å), and on the right, natural charges for C^1, C^2, and C^3. Parameter *A* is defined as the ratio of bond distances $(C^1-C^2)/(C^2-C^3)$ and correlates to the polarization of the π-electrons along the delocalized $C^1-C^2-C^3$ system. **b**, A comparison with gold alkylidene **7** showing the relative natural orbital populations of σ and π contributions to the gold–carbon bond. Calculated bond distances (Å) for **7** are shown on the right.

substituents ($A = 0.955$) and even further for ester-substituted substrate **6** ($A = 0.983$). The corresponding gold-coordinated structures $\mathbf{Au_O^{PMe}}$, $\mathbf{Au_{Me}^{PMe}}$ and $\mathbf{Au_E^{PMe}}$ all show increased *A* values as a result of the ability of the gold moiety to stabilize positive charge at C^1. In $\mathbf{Au_{Me}^{PMe}}$, *A* is close to 1 (0.993), suggesting that a secondary gold-stabilized carbocation is as stabilized as a tertiary carbocation. For the diester-substituted allyl carbene $\mathbf{Au_E^{PMe}}$, the π-system is now polarized towards the electron-deficient C^3 leading to $A = 1.029$. Importantly, the magnitude of stabilization from the gold moiety grows with increasing electrophilicity of the allyl cation. This conclusion can also be reached by considering the natural atomic charge on C^3. This charge is essentially unaffected in **4** (0.86) compared with $\mathbf{Au_O^{PMe}}$ (0.83), whereas it is significantly reduced in **5** (0.43) compared with $\mathbf{Au_{Me}^{PMe}}$ (0.34), and in **6** (0.21) compared with $\mathbf{Au_E^{PMe}}$ (0.10).

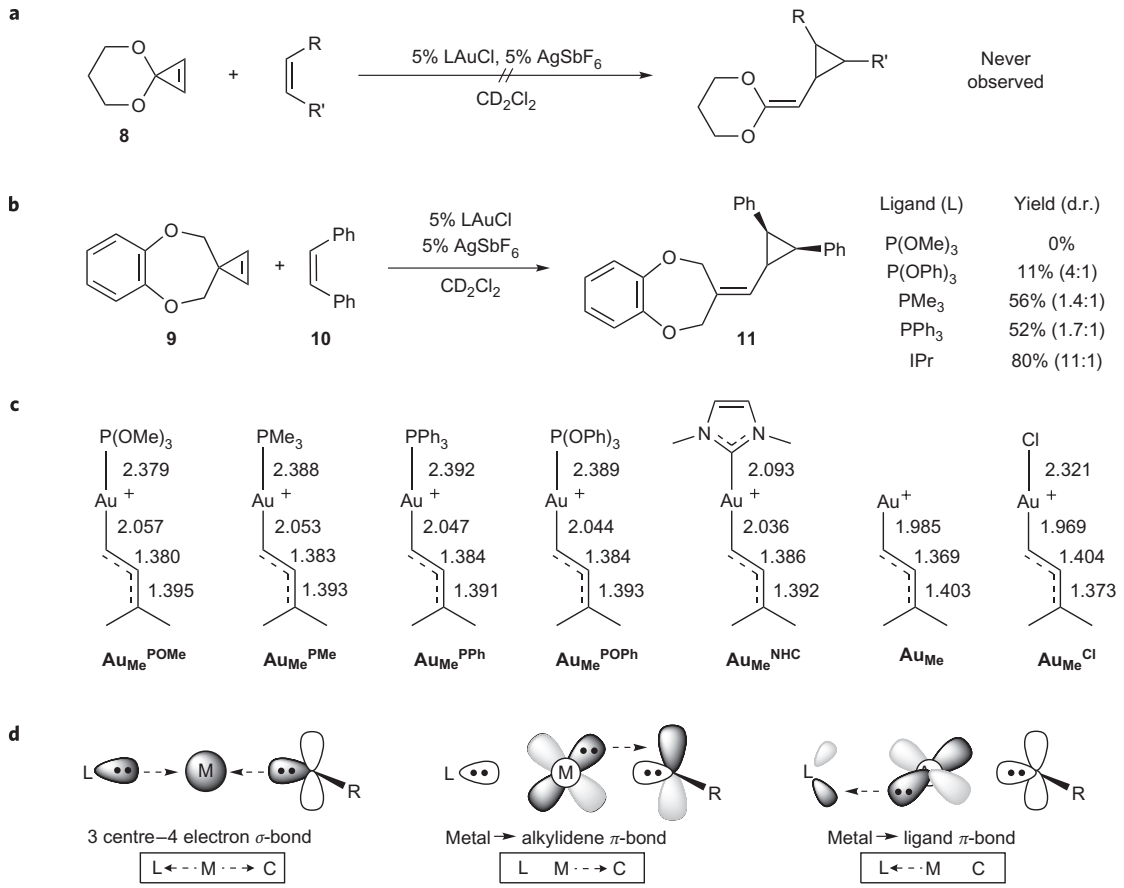

Figure 3 | Experimental and theoretical comparison for the carbene reactivity of the substrate with different ancillary ligands. a,**b**, Attempted (**a**) and observed (**b**) carbene-like reactivity, demonstrating the impact of the ancillary ligand on the yield of cyclopropanation product. **c**, Bond distances in $Au_{Me}{}^{L}$ complexes. **d**, A stylized depiction of the most important bonding interactions in L–Au(I)–$CR_2{}^{+}$ species. d.r., diastereomeric ratio.

In order to examine the bonding and reactivity of non-vinylic gold(I) intermediates, we also examined gold alkylidene **7** and compared it to the gold vinylic carbene species (Fig. 2b). Our results show that the gold–carbon bond distance (2.057 Å) varies little from the vinyl carbenes. However, in the absence of a delocalized neighbouring vinyl group, the gold–carbon bond possesses more π-character, with decreased σ-donation from alkylidene to gold[24]. This demonstrates the ability of the gold moiety to stabilize carbenes of varying electrophilicity by modulating the nature of the gold–carbon bond.

A direct consequence of the differences between $\mathbf{Au_O}^{\mathbf{PMe}}$ and $\mathbf{Au_{Me}}^{\mathbf{PMe}}$ is the increased barrier to C^2-C^3 bond rotation in $\mathbf{Au_{Me}}^{\mathbf{PMe}}$ (Fig. 1). In addition, a difference in reactivity could be expected: $\mathbf{Au_O}^{\mathbf{PMe}}$ may react as a gold-stabilized carbocation, whereas $\mathbf{Au_{Me}}^{\mathbf{PMe}}$ may react more as a gold-stabilized carbene. We tested and confirmed this hypothesis experimentally. We were unable to observe productive cyclopropanation of intermediates resulting from the gold-catalysed reaction of cyclopropene **8** (as a precursor to $\mathbf{Au_O}^{\mathbf{PMe}}$, Fig. 3a). However, the gold-catalysed reaction of cyclopropene **9** (which should decompose to an intermediate similar to $\mathbf{Au_{Me}}^{\mathbf{PMe}}$) with *cis*-stilbene provided the product of stereospecific olefin cyclopropanation (Fig. 3b). As the yield of this reaction was highly dependent on the ancillary ligand, we next examined the effect of this ligand on the nature of the $Au-C^1$ bond.

Impact of the ligand[1,25]. The computed structures of $Au_{Me}{}^{L}$, for various ligands (L) are shown in Fig. 3c. The L–Au$-C^1$ bonding network can be partitioned into three components (Fig. 3d)[26,27]. Because there is only one vacant valence orbital on gold (6*s*), the Pauli exclusion principle tells us that a three-centre–four-electron σ-hyperbond[28] (where hyperbond refers to bonding beyond the reduced 12-electron valence space) must be formed for the P$-$Au$-$C triad as [P:Au$-$C$\leftrightarrow$P$-$Au:C] (or C$-$Au$-$C triad for the NHC ligand). As a result, the $Au-C^1$ bond order decreases with increasing *trans* ligand σ-donation (*trans* influence). In the absence of a *trans* ligand, the Au–C bond in $\mathbf{Au_{Me}}$ is notably shorter (1.985 Å), whereas, in $\mathbf{Au_{Me}}^{\mathbf{PMe}}$, the electron-donating PMe_3 (strong *trans* influence) results in a correspondingly long $Au-C^1$ bond length of 2.053 Å.

In addition, the metal centre is able to form two π-bonds by donation from perpendicular filled *d*-orbitals into empty π-acceptors on the ligand and C^1. Although these two bonds are not mutually exclusive, they compete for electron density from gold. As a result, strongly π-acidic ligands decrease back-donation to the substrate, resulting in even longer $Au-C^1$ bonds (2.057 Å for $\mathbf{Au_{Me}}^{\mathbf{POMe}}$). In contrast, the π-donating chloride ligand in $\mathbf{Au_{Me}}^{\mathbf{Cl}}$ increases back-donation to C^1 resulting in a very short gold$-$carbon bond (1.969 Å). In general, the strength of the back-donation to C^1 is dependent on both ligand and (as demonstrated in the previous section) the electrophilicity of the π-acceptor on C^1.

Table 1 | Calculated natural populations (charge) for the ancillary ligand, gold atom and substrate.

	$Au_{Me}{}^{NHC}$	$Au_{Me}{}^{PMe}$	$Au_{Me}{}^{POMe}$	$Au_{O}{}^{NHC}$	$Au_{O}{}^{PMe}$	$Au_{O}{}^{POMe}$
Ligand	0.32	0.40	0.45	0.31	0.37	0.42
Metal	0.39	0.30	0.25	0.36	0.27	0.23
Substrate	0.29	0.31	0.31	0.33	0.36	0.35

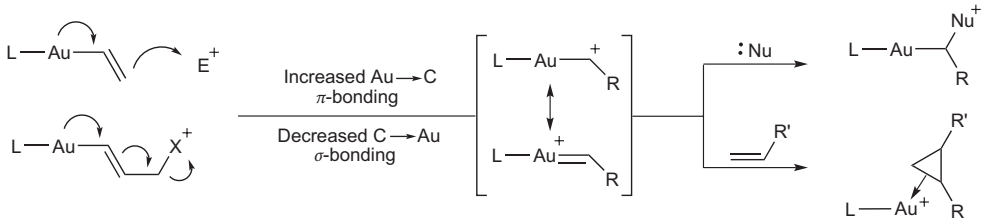

Figure 4 | Arrow pushing in the formation of gold-stabilized carbenes. Such arrow pushing is a useful mnemonic for keeping track of electrons, but it can lead to misconceptions about bonding. Although the gold–carbon bond in the intermediate carbene has both σ and π components, the overall bond order is generally less than or equal to one.

The impact of these changes on reactivity is directly apparent in the yield of the cyclopropanation product (Fig. 3b). π-acidic ligands are expected to increase carbocation-like reactivity by decreasing gold-to-C^1 π-donation. Accordingly, we found that strongly π-acidic phosphite ligands provide only traces of the desired product and significant polymerization. Conversely, ligands that increase gold-to-C^1 π-donation are expected to reduce carbocation-like reactivity, whereas those ligands that decrease C^1-to-gold σ-donation should increase carbene-like reactivity. The *N*-heterocyclic ligand IPr (1,3-bis(2,6-diisopropylphenyl)imidazol-2-ylidene) should therefore affect both of these changes (it is strongly σ-donating and only weakly π-acidic). This was reflected by our results, in which $IPrAu^+$ gave the product of stereospecific cyclopropanation in excellent yield and with high diastereoselectivity (80% yield, 11:1 *cis*:*trans*). Phosphine ligands fell in between these two extremes. Finally, AuCl was unreactive under these conditions.

Charge distribution. In order to provide a better and more general view of the bonding in gold vinyl carbene species, we calculated natural charge distributions for the ligand, gold and substrate using natural bond orbital analyses. Table 1 shows that the charge is relatively equally distributed between the substrate, gold and the ligand. Across the $\mathbf{Au_{Me}}^{\mathbf{L}}$ and $\mathbf{Au_O}^{\mathbf{L}}$ series, the charge on the ligand and the gold is well correlated: an increase in ligand charge is associated with a similar decrease in charge on the gold, but these changes have little effect on the charge on the substrate. However, changing the substrate from $\mathbf{Au_{Me}}^{\mathbf{L}}$ to $\mathbf{Au_O}^{\mathbf{L}}$ results in an increase in substrate charge. This correlates with a decrease in the charges on both the gold and the ligand. These results again demonstrate that both the ligand and the substrate play important roles in determining the overall electronic structure.

Bonding and reactivity. The model in Fig. 3d for bonding in gold-stabilized carbenes proposes that these intermediates possess highly electron-deficient α-carbons that are stabilized, to varying degrees, by back-donation from the metal to the vacant $p\pi$-orbital of the singlet carbene. This electron deficiency reduces donation from the filled sp^2 σ-orbital of the carbene to the metal, therefore minimizing gold–carbon σ-bonding. Thus, our model suggests that the conversion of a vinylgold intermediate into a gold-stabilized carbene, which is commonly proposed in gold-catalysed reactions[29–34], occurs with an increase in gold–carbon π-bonding and a decrease in the σ-bonding (Fig. 4). The bonding situation in these carbene intermediates has often been depicted by two extreme resonance structures: a carbocation with a gold–carbon single bond or a carbene with a gold–carbon double bond. Much like the double 'half-bond' model proposed for rhodium carbenoid intermediates[35,36], the depiction of a gold-stabilized carbene with a gold–carbon double bond should not be taken as an indication of a bond order of two, but rather a means to convey that both σ and π components to the bond are present. To illustrate this, we calculated gold–carbon natural bond orders for $\mathbf{Au_O}^{\mathbf{PMe}}$ (0.53), $\mathbf{Au_{Me}}^{\mathbf{PMe}}$ (0.91), and **7** (1.14). Nucleophilic attack on the now highly electrophilic $p\pi$-orbital of the carbon adjacent to gold restores the gold–carbon σ-bond[37–39]. In this scenario, divergence towards carbocation-like or carbene-like reactivity may also be influenced by the potential of the nucleophile to intercept the developing positive charge. Alternatively, gold-stabilized carbene intermediates may react with concerted carbene-like reactivity (for example, as in cyclopropanation), especially when the gold is coordinated to electron-donating ligands.

Conclusions

We suggest that the reactivity in gold(I)-coordinated carbenes is best accounted for by a continuum ranging from a metal-stabilized singlet carbene to a metal-coordinated carbocation. The position of a given gold species on this continuum is largely determined by the carbene substituents and the ancillary ligand. Consideration of the bonding description described herein provides insight into previously reported gold-catalysed transformations and a basis for the *ab initio* prediction of reactivity, optimization of ligand effects and design of new gold-catalysed reactions.

Methods

Calculations were performed using density functional theory with the M06 functional, as implemented in Jaguar 7.6[40]. All calculations used the Hay and Wadt small core–valence relativistic effective core potential[41]. The LACVP** basis set was used for all geometry optimizations and LACV3P ++**(2*f*) for energies. LACV3P ++**(2*f*) uses the LACV3P++** basis set as implemented in Jaguar plus a double-zeta *f*-shell with exponents from Martin and Sundermann[42]. All electrons were described for all other atoms using the 6-31G** or 6-311 ++G** basis sets[43,44]. For each optimized structure, the M06 analytic Hessian was calculated to obtain the vibrational frequencies, which in turn were used to obtain the zero-point energies and free energy corrections (without translational or rotational components). Solvent corrections were based on single-point self-consistent Poisson–Boltzmann continuum solvation calculations for CH_2Cl_2 ($\varepsilon = 8.93$ and $R_0 = 2.33$ Å using the PBF[45] module in Jaguar.

Received 1 June 2009; accepted 14 July 2009;
published online 16 August 2009

References

1. Gorin, D. J., Sherry, B. D. & Toste, F. D. Ligand effects in homogeneous Au catalysis. *Chem. Rev.* **108,** 3351–3378 (2008).
2. Hashmi, A. S. K. Gold-catalyzed organic reactions. *Chem. Rev.* **107,** 3180–3211 (2007).
3. Fürstner, A. & Davies, P. W. Catalytic carbophilic activation: catalysis by platinum and gold π acids. *Angew. Chem. Int. Ed.* **46,** 3410–3449 (2008).
4. Jiménez-Núñez, E. & Echavarren, A. M. Gold-catalyzed cycloisomerizations of enynes: a mechanistic perspective. *Chem. Rev.* **108,** 3326–3350 (2008).
5. Gorin, D. J. & Toste, F. D. Relativistic effects in homogeneous gold catalysis. *Nature* **446,** 395–403 (2007).
6. Fedorov, A., Moret, M. E. & Chen, P. Gas-phase synthesis and reactivity of a gold carbene complex. *J. Am. Chem. Soc.* **130,** 8880–8881 (2008).
7. Hashmi, A. S. K. High noon in gold catalysis: Carbene versus carbocation intermediates. *Angew. Chem. Int. Ed.* **47,** 6754–6756 (2008).
8. Correa, A. *et al.* Golden carousel in catalysis: the cationic gold/propargylic ester cycle. *Angew. Chem. Int. Ed.* **47,** 718–721 (2008).
9. Fürstner, A. & Morency, L. On the nature of the reactive intermediates in gold-catalyzed cycloisomerization reactions. *Angew. Chem. Int. Ed.* **47,** 5030–5033 (2008).

10. Seidel, G., Mynott, R. & Fürstner, A. Elementary steps of gold catalysis: NMR spectroscopy reveals the highly cationic character of a "gold carbenoid." *Angew. Chem. Int. Ed.* **48,** 2510–2513 (2009).
11. Johansson, M. J., Gorin, D. J., Staben, S. T. & Toste, F. D. Gold(I)-catalyzed stereoselective olefin cyclopropanation. *J. Am. Chem. Soc.* **127,** 18002–18003 (2005).
12. Horino, Y., Yamamoto, T., Ueda, K., Kuroda, S. & Toste, F. D. Au(I)-catalyzed cycloisomerizations terminated by sp^3 C–H bond insertion. *J. Am. Chem. Soc.* **131,** 2809–2811 (2009).
13. Lemière, G. *et al.* Generation and trapping of cyclopentenylidene gold species: four pathways to polycyclic compounds. *J. Am. Chem. Soc.* **131,** 2993–3006 (2009).
14. Fructos, M. R. *et al.* A gold catalyst for carbene-transfer reactions from ethyl diazoacetate. *Angew. Chem. Int. Ed.* **44,** 5284–5288 (2005).
15. López, S., Herrero-Gómez, E., Pérez-Galán, P., Nieto-Oberhuber, C. & Echavarren, A. M. Gold(I)-catalyzed intermolecular cyclopropanation of enynes with alkenes: trapping of two different gold carbenes. *Angew. Chem. Int. Ed.* **45,** 6029–6032 (2005).
16. Fedorov, A. & Chen, P. Electronic effects in the reactions of olefin-coordinated gold carbene complexes. *Organometallics* **28,** 1278–1281 (2009).
17. Sheehan, S. M., Padwa, A. & Snyder, J. P. Dirhodium(II) tetracarboxylate carbenoids as catalytic intermediates. *Tetrahedron Lett.* **39,** 949–952 (1998).
18. Doyle, M. P. Electrophilic metal carbenes as reaction intermediates in catalytic reactions. *Acc. Chem. Res.* **19,** 348–356 (1986).
19. Nowlan, D. T., Gregg, T. M., Davies, H. M. L. & Singleton, D. A. Isotope effects and the nature of selectivity in rhodium-catalyzed cyclopropanations. *J. Am. Chem. Soc.* **125,** 15902–15911 (2004).
20. Zhao, Y. & Truhlar, D. G., Density functionals with broad applicability in chemistry. *Acc. Chem. Res.* **41,** 157–167 (2008).
21. Truhlar, D. G. Molecular modeling of complex chemical systems. *J. Am. Chem. Soc.* **130,** 16824–16827 (2008).
22. Zhao, Y. & Truhlar, D. G. Benchmark energetic data in a model system for Grubbs II metathesis catalysis and their use for the development, assessment, and validation of electronic structure methods. *J. Chem. Theory Comput.* **5,** 324–333 (2009).
23. Reed, A. E., Curtiss, L. A. & Weinhold, F. Intermolecular interactions from a natural bond orbital, donor-acceptor viewpoint. *Chem. Rev.* **88,** 899–926 (1988).
24. Irikura, K. K. & Goddard III, W. A. Energetics of third-row transition metal methylidene ions MCH_2^+ (M = La, Hf, Ta, W, Re, Os, Ir, Pt, Au). *J. Am. Chem. Soc.* **116,** 8733–8740 (1994).
25. Padwa, A. & Austin, D. J. Ligand effects on the chemoselectivity of transition metal catalyzed reactions of α-diazo carbonyl compounds. *Angew. Chem. Int. Ed. Engl.* **33,** 1797–1815 (1994).
26. Dewar, M. A review of the π-complex theory. *Bull. Soc. Chim. Fr.* **18,** C71–C77 (1951).
27. Chatt, J. & Duncanson L. A. Olefin co-ordination compounds. Part III. Infra-red spectra and structure: attempted preparation of acetylene complexes. *J. Chem. Soc.* 2939–2947 (1953).
28. Landis, C. R. & Weinhold, F. Valence and extra-valence orbitals in main group and transition metal bonding. *J. Comput. Chem.* **28,** 198–203 (2007).
29. Mamane, V., Gress, T., Krause, H. & Fürstner, A. Platinum- and gold-catalyzed cycloisomerization reactions of hydroxylated enynes. *J. Am. Chem. Soc.* **126,** 8654–8655 (2004).
30. Luzung, M. R., Markham, J. P. & Toste, F. D. Catalytic isomerization of 1,5-enynes to bicyclo[3.1.0]hexenes. *J. Am. Chem. Soc.* **126,** 10858–10859 (2004).
31. Gorin, D. J. Davis, N. R. & Toste, F. D. Gold(I)-catalyzed intramolecular acetylenic Schmidt reaction. *J. Am. Chem. Soc.* **127,** 1126–1127 (2005).
32. Nieto-Oberhuber, C., Muñoz, M. P., Buñuel, E., Nevado, C., Cárdenas, D. J. & Echavarren, A. M. Cationic gold(I) complexes: highly alkynophilic catalysts for the exo- and endo-cyclization of enynes. *Angew. Chem. Int. Ed.* **43,** 2402–2406 (2004).
33. Shapiro, N. D. & Toste, F. D. Rearrangement of alkynyl sulfoxides catalyzed by gold(I) complexes. *J. Am. Chem. Soc.* **129,** 4160–4161 (2007).
34. Zhang, G. & Zhang, L. Au-containing all-carbon 1,3-dipoles: generation and [3 + 2] cycloaddition reactions. *J. Am. Chem. Soc.* **130,** 12598–12599 (2008).
35. Snyder, J. P. *et al.* A stable dirhodium tetracarboxylate carbenoid: crystal structure, bonding analysis, and catalysis. *J. Am. Chem. Soc.* **123,** 11318–11319 (2001).
36. Costantino, G., Rovito, R., Macchiarulo, A. & Pellicciari, R. Structure of metal–carbenoid intermediates derived from the dirhodium(II)tetracarboxylate mediated decomposition of α-diazocarbonyl compounds: a DFT study. *J. Mol. Struct. Theochem*, **581,** 111 (2002).
37. Amijs, C. H. M., López-Carrillo, V. & Echavarren, A. M. Gold-catalyzed addition of carbon nucleophiles to propargyl carboxylates. *Org. Lett.* **9,** 4021–4024 (2007).
38. Davies, P. W. Albrecht, S. J.-C. Alkynes as masked ylides: gold-catalysed intermolecular reactions of propargylic carboxylates with sulfides. *Chem. Commun.* 238–240 (2008).
39. Nieto-Oberhuber, C. *et al.* Gold(I)-catalyzed cyclizations of 1,6-enynes: alkoxycyclizations and exo/endo skeletal rearrangements. *Chem. Eur. J.* **12,** 1677–1693 (2006).
40. Jaguar 7.6 (Schrodinger, New York, 2006).
41. Hay, P. J. & Wadt, W. R. Ab initio effective core potentials for molecular calculations—potentials for K to Au including the outermost core orbitals. *J. Chem. Phys.* **82,** 299–310 (1985).
42. Martin, J. M. L. & Sundermann, A. Correlation consistent valence basis sets for use with the Stuttgart-Dresden-Bonn relativistic effective core potentials: The atoms Ga-Kr and In-Xe. *J. Chem. Phys.* **114,** 3408–3420 (2001).
43. Krishnan, R., Binkley, J. S., Seeger, R. & Pople, J. A. Self-consistent molecular-orbital methods. XX. A basis set for correlated wave-functions. *J. Chem. Phys.* **72,** 650–654 (1980).
44. Frisch, M. J., Pople, J. A. & Binkley, J. S. Self-consistent molecular-orbital methods 25. Supplementary functions for Gaussian-basis sets. *J. Chem. Phys.* **80,** 3265–3269 (1984).
45. Tannor, D. J. *et al.* Accurate first principles calculation of molecular charge-distributions and solvation energies from ab-initio quantum-mechanics and continuum dielectric theory. *J. Am. Chem. Soc.* **116,** 11875–11882 (1994).

Acknowledgements

F.D.T. acknowledges NIHGMS, Bristol-Myers Squibb and Novartis for funding, and J. Matthey for the donation of $AuCl_3$. The MSC computational facilities were funded by grants from ARO-DURIP and ONR-DURIP. D.B. and E.T. thank R. Nielsen for useful suggestions.

Author contributions

D.B., N.D.S. and F.D.T. originated the idea and wrote the manuscript, N.D.S. and Y.W. performed the experiments, D.B. and E.T. performed the calculations, all authors contributed to discussions and edited the manuscript. D.B. and N.D.S. contributed equally to this work.

Additional information

Supplementary information and chemical compound information accompany this paper at www.nature.com/naturechemistry. Reprints and permission information is available online at http://npg.nature.com/reprintsandpermissions/. Correspondence and requests for materials should be addressed to F.D.T.